Journal of Pure Applied and Industrial Physics, *Vol.8(9),98-106, September 2018* *ISSN 2229-7596 (Print)*
(An International Research Journal), *IF = 4.715, www.physics-journal.org* *ISSN 2319-7617 (Online)*

Effect of CTAB Concentration on the Morphology of Manganese Oxide Nanostructures

B. D. Biswas[1], M. D. Purkayastha[1] and T. Pal Majumder[1*]

[1]Department of Physics,
University of Kalyani, Kalyani-741235, West Bengal, INDIA.
email: sujatab88@gmail.com; borahmou@gmail.com.
*Corresponding author email: tpmajumder1966@gmail.com.

(Received on: September 1, 2018)

ABSTRACT

In this work, the effect of concentration of cetyltrimethylammonium bromide (CTAB) in the synthesis of manganese oxide (Mn_2O_3) nanostructures has been investigated adopting the hydrothermal route. The products were characterized by XRD, infrared spectroscopy (FTIR) and scanning electron microscopy (SEM). XRD confirming the formation of Mn_2O_3 shows an intense diffraction peak at 36° with lattice plane (2 0 3). The IR spectra shows characteristic peaks at 489, 612 cm^{-1} corresponding to O-Mn-O bonds. With the increase in CTAB amounts from 20 mg to100 mg, the morphology changes from spherical to rod-like. Change in morphology could presumably lead to change in properties and make Mn_2O_3 nanostructures ideal candidates for photocatalytic, supercapacitor, battery and fuel cell applications.

Keywords: CTAB; Morphology; Manganese oxides; Nanostructures; Optical behavior.

1. INTRODUCTION

Transition metal oxide nanoparticles epitomize an industrially important class of nanomaterials because of their unique physio-chemical properties. It is the morphology of the particles that plays a vital role in deciding the application for which it is suitable. Particularly, the one-dimensional nanoparticles have immense technological applications owing to their excellent electrochemical properties, cost effectiveness, easy preparation techniques and environmental benign nature[1-3]. Tuning of morphology requires the use of surfactants. Surfactants are known to have a hydrophilic head and a hydrophobic tail. They can easily assemble into well-defined structures and accordingly provide the template for the synthesis of the nanomaterial. Of the various synthetic routes, the hydrothermal route using surfactants is the most promising as it can effectively

control the phase and morphology of the nanoparticles. Also, it can generate highly crystalline, pure nanoparticles with low aggregation and narrow size distribution[4]. Recently, manganese oxides are being considered for numerous applications. This is because manganese has the ability to form bonds with oxygen in multiple valence states. Both solvothermal and hydrothermal routes are being employed nowadays for the synthesis of manganese oxides even without the use of templates and surfactants[5]. However, there are several parameters as temperature and aging time that can influence the growth of nanoparticles in the solution those had been adopted as the synthesis route[6]. Hence, the controlled synthesis of manganese oxide nanoparticles with favorable surface morphology, good crystallinity, phase structure and high reproducibility still remains a great challenge.

This paper reports the controlled synthesis of Mn_2O_3 nanoparticles via a mild hydrothermal route with the use of CTAB surfactant. Mn_2O_3 is a typical p-type semiconductor that has implicit applications in solar cells, sensors, lithium ion batteries and cathodic electrocatalysts[7-10]. The effects of change in CTAB concentration on the evolution of phase and structural morphology of Mn_2O_3 nanoparticles were investigated. Also, the effects of CTAB on photoluminescence properties of the nanoparticles were investigated.

2. MATERIALS AND METHODS

2.1 Materials for synthesis

Anal grade chemicals were used as received commercially without further purification. Manganese acetate tetrahydrate, sodium hydroxide (NaOH) pellets were obtained from Merck, Germany. Cetyltrimethylammonium bromide (CTAB) was obtained from Loba Chemie. Doubly distilled water was used in all experiments.

2.2 Sample preparation

In a typical procedure to synthesize Manganese oxide nanoparticles (Mn_2O_3), 0.01 mole (approximately 2.456 g) of manganese acetate tetrahydrate was dissolved in 30mL distilled de-ionized water. After stirring for about 30 minutes, an aqueous solution of NaOH prepared by dissolving 0.02 mole (approximately 0.799 g) of NaOH pellets in 20 ml distilled de-ionized water was added drop wise. The two were reacted each other to produce a precipitation of $Mn(OH)_2$.. An aqueous micelle solution of CTAB (20 mg in 30 mL distilled de-ionized water) was also added to the mixed solution under magnetic stirring at 80ºC. The reaction was continued till the volume of the slurry decreased appreciably. The colour of the residue was brownish at this stage at the end of that. Then the solution was put into a Teflon lined stainless steel autoclave which was maintained at an average of 180 ^{0}C for 12 hours, and then it allowed to naturally cool down to room temperature. The resulting brownish precipitate was obtained after it filtered which was washed subsequently for several times with double distilled de-ionized water and absolute ethanol and after that it was dried in air at 65 ^{0}C for 3 hours. To obtain a recognizable change which has been visibly observed in the morphology of

the structure, the same experiment was repeated with the variation of the concentration of CTAB such as 50mg and 100 mg and ultimately the required nanorods were observed after confirming it from scanning electron micrograph (SEM). The aforesaid experiment was also repeated without the addition of CTAB to obtain normal Mn_2O_3 for the purposes of comparison.

2.3 Sample characterization

The as-synthesized product was characterized by an X'Pert PRO PANalytical X-ray diffractometer (XRD) using CuKα radiation (wavelength λ= 0.15418 nm) at an accelerating voltage and applied current of 30 kV and 20 mA, respectively to identify the resultant phase and crystal structure of the synthesized powder. The data was collected with a step of 0.02° in the range of 2θ from 10° to 80°. The chemical identity of the product was determined by comparing the experimental X-ray powder patterns to standards compiled by the Joint Committee on Powder Diffraction and Standards (JCPDS). UV-vis absorption spectra were obtained with a UV 3600 spectrophotometer in the range from 200 to 800 nm. Identification of functional groups in the sample was studied with a FT-IR spectrophotometer Perkin Elmer (Spectrum one L120-000A). Photoluminescence (PL) emission spectrum was obtained by employing an excitation wavelength of 280 nm using PTI QM 40 spectrophotometer. Morphology, elemental analysis of the synthesized nanomaterial was investigated by a SEM device coupled with EDX (Energy dispersive X-ray spectroscopy).

3. RESULTS AND DISCUSSION

3.1 XRD and EDS

The diffraction pattern of all the samples (Fig.1) well coincided with the tetragonal manganese oxide corresponding to the diffraction planes (111), (202), (221), (203), (213), (204), (105), (510) and (305) supported by JCPDS card no. 06-0540. The nano powder exhibited brownish hue and the crystallite size was calculated from the peak widths using the Scherer equation (1)[11]

$$D = \frac{K\lambda}{\beta \operatorname{Cos}\theta} \tag{1}$$

where K is a dimensionless shape factor that varies with the actual shape of the crystallite, λ is the X-ray wavelength λ= 1.5418 Å, β is the line broadening at half the maximum intensity (FWHM) and θ is Bragg's angle. It was observed that the crystallite size decreases with the increase of CTAB concentration in the order of 34, 27, 25 and 13 nm, respectively for the amount of CTAB being employed varying from 0, 20, 50, 100 mg, respectively.

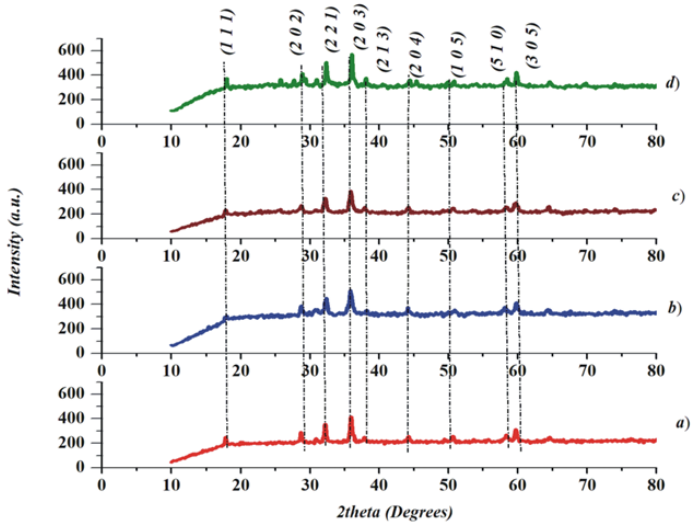

Figure1. XRD of synthesized Mn_2O_3 with the variation of the concentration of CTAB (a) 0 mg, (b) 20 mg, (c) 50 mg and (d) 100 mg.

Energy dispersive X ray spectroscopy (EDS) analysis of the synthesized Mn_2O_3 without the addition of CTAB (Fig.2), obtained from different peak areas of the sample shows the presence of Manganese at 6 KeV and Oxygen in the range of 0-1 KeV [12]. Furthermore, neither N nor C signals were detected in the EDS spectrum which means that the product is pure and free of any surfactant or impurity. The composition data (at % and wt %) of Mn_2O_3 is given in table1.

Table 1: EDS: composition data

Element	Weight %	Atomic %
Oxygen (O)	10.21	28.07
Manganese (Mn)	89.79	71.93

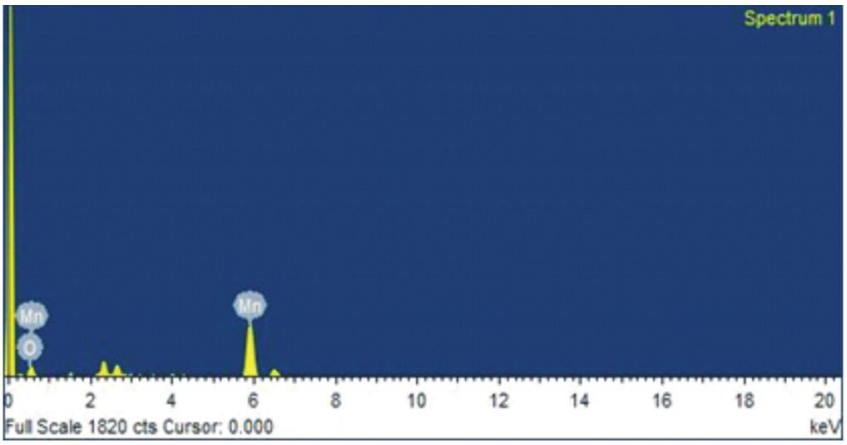

Figure 2. EDS spectra of Mn_2O_3 without CTAB indicating elemental composition.

3.2 Morphology

The morphology of Mn_2O_3 nanoparticles was investigated at a magnification of 200 nm using SEM (Fig.3). The SEM images of Mn_2O_3 without the addition of CTAB (Figure 3a) were spherical agglomerates. However, as addition of 20 mg of CTAB in the preparation the morphological pattern showed a clear picture of spherical nanoparticles as depicted from Figure 3a. With further addition of CTAB (50 mg) (Figure 3c) the diameter of the nanospheres was seen to increase. Finally, when the amount of CTAB was 100 mg, beautiful rod-like nanostructures (Figure 3d) were visible. This could be attributed to the linear arrangement of the nanospheres to form rod-like structures. The particle size is seen to vary from 1µm to 200 nm. There arises a discrepancy in the particle sizes as measured by XRD and SEM which implies that the particles must have coalesced. This tends to reduce the benefits of large interfacial area between the particles[13].

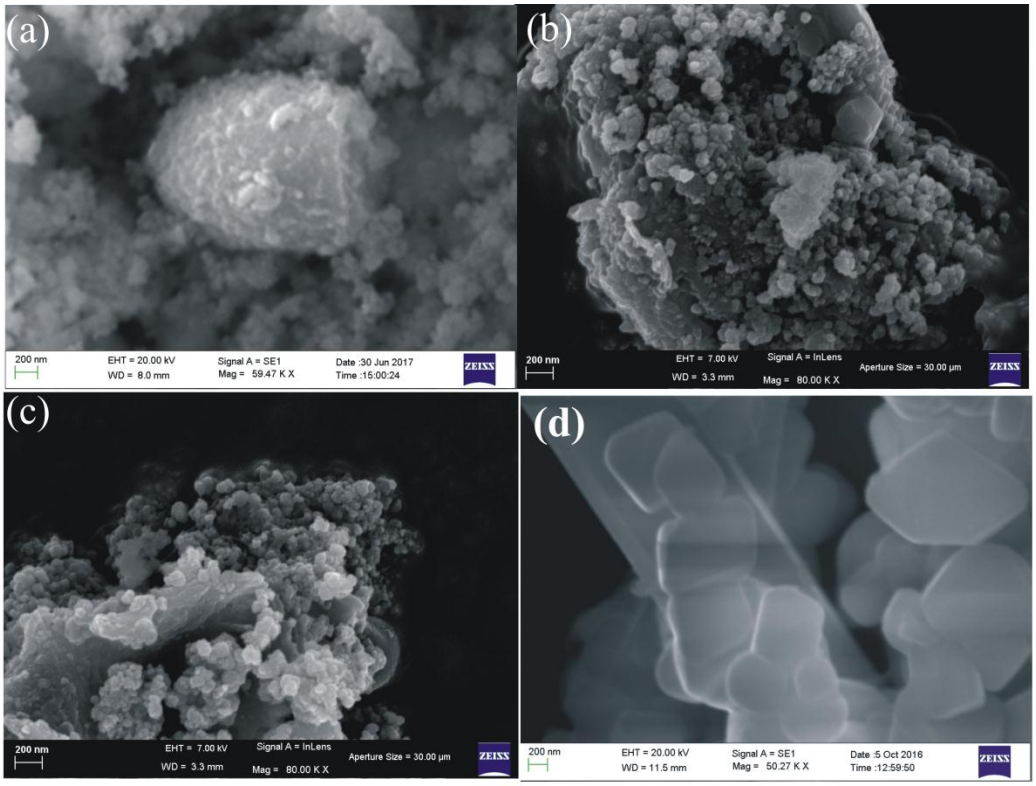

Figure 3. SEM image of Mn_2O_3 at 200 nm magnification 59.99 K X with CTAB variation (a) 0 mg, (b) 20 mg, (c) 50 mg and (d) 100 mg.

3.3 UV-vis spectra

Light absorbing properties are crucial in interpreting the behavior of the nanoparticles. Figure 4 shows the UV-vis absorption spectra of Mn_2O_3 without CTAB with a sharp peak at

276 nm. The peak appeared red shifted to 300, 305, 313 nm, respectively with the variation of amount of CTAB from 20, 50 and 100 mg. The optical band gap was calculated using the Tauc relation (2) from the absorption spectrum[14].

$$\alpha h\nu = C(h\nu - E_g)^n \quad (2)$$

where C is a constant, α is molar extinction coefficient, E_g is the band gap energy of the material and n determines the type of transition. When n=1/2, E_g will denote the direct allowed band gap. The value of E_g was estimated from the intercept of the linear portion of $(\alpha h\nu)^2$ versus hν plot on the hν axis as in Figure 4 (inset). The values of band gap were found to decrease with the increase in CTAB amounts. The values were estimated as 3.86, 3.84, 3.7 and 3.57 eV for the different proportionate of the amount of CTAB from 0, 20, 50 and 100 mg, respectively. These values predict semiconducting nature of the samples. However the values are lower than those reported by other researchers[15]. This lowering may be caused by structural distortion associated with the lower order due to oxygen deficiency in the samples[15]. Thus, band gap values can be tuned effectively by varying the amount of CTAB.

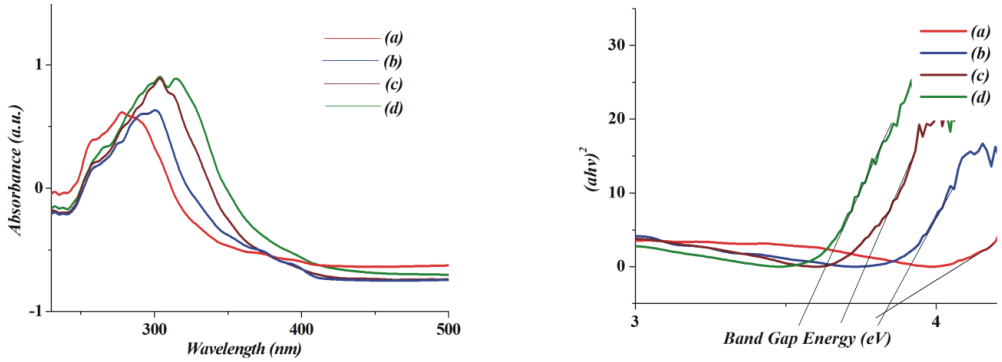

Figure 4. UV-visible spectra of Mn_2O_3 with the variation of amount of CTAB (a) 0 mg, (b) 20 mg, (c) 50 mg and (d) 100 mg (inset) Tauc plot indicating band gap.

3.4 FTIR

The FT-IR spectra of Mn_2O_3 prepared with different amounts of CTAB has been illustrated in Fig.5. On examining the spectra obtained after spectral scanning, and focusing on the frequently used portion between 400 and 4000 cm^{-1}, the bands emerging in relation to stretching collision of O-Mn-O were observed at 489 and 612 cm^{-1} [16]. The band at 1111 cm^{-1} corresponds to Mn-OH bending vibration. The peak at 1622 cm^{-1} symbolizes the bending collision of adsorbed water. The broad band centered at 3400 cm^{-1} signifies the stretching collision of H-O-H bonds and hydroxyl absorption[12]. There is no significant peak has been noticed due to the introduction of CTAB in the preparation with varying their concentration. However, absorption intensity has been changed because of morphological variation of structures of the prepared nanostructures influenced by CTAB concentration. The absorption intensity increases monotonically with the increase of concentration of CTAB in the preparation. So, the presence of CTAB in the preparation solution has produced an efficient

electrostatic interaction in the structures which allowed more absorption of radiation based on their characteristic frequency of the prepared Mn_2O_3 nanostructures. Except that it also influence the respectic dangling bond in the prepared system significantly.

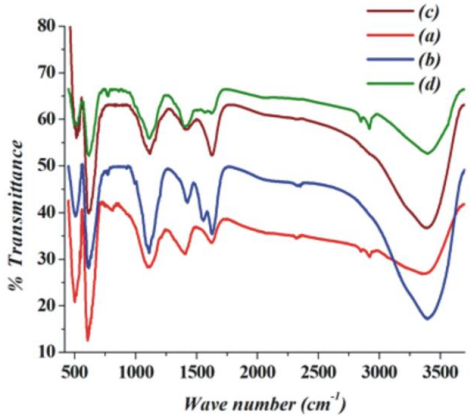

Figure 5. FT-IR spectra of Mn_2O_3 with CTAB variation (a) 0 mg, (b) 20 mg, (c) 50 mg and (d) 100 mg.

3.5 PL spectra

The room temperature PL emission spectrum was recorded by employing an excitation wavelength of 280 nm (Figure 6).The spectrum showed peaks at 408 nm and 432 nm. The emission intensity of Mn_2O_3 without CTAB was found to be high. Intensity at first increased with the addition of 20 mg CTAB but further increase (50 mg, 100 mg) caused emission quenching. The emission in the visible region of the electromagnetic spectrum may be ascribed to oxygen vacancies and intrinsic defects. These results are red shifted in comparison to those reported by Pandey et al for nanorods[17]. This implied that with the use of requisite amount of CTAB, the electron hole pairs could be efficiently separated and inhibited from recombining so it significantly contribute to the electrostatic interaction as a whole and at the same time the respective dangling bond influenced significantly which we already mentioned in the observation of FTIR spectra. This in turn predicts efficient photocatalysis.

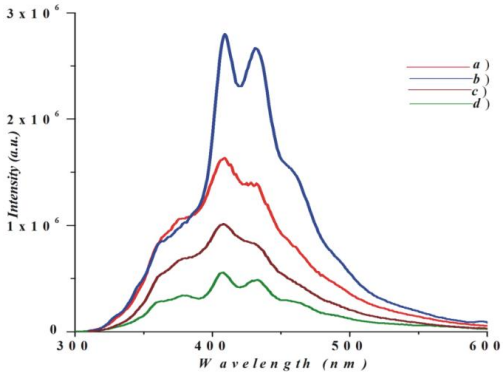

Figure 6. PLspectra of Mn_2O_3 with CTAB variation (a) 0 mg, (b) 20 mg, (c) 50 mg and (d) 100 mg.

4. CONCLUSIONS

In the present study, we have successfully synthesized Mn_2O_3 nanostructures with varied morphology simply by changing the amounts of CTAB in the reaction mixture. X- ray diffraction studies confirmed that the synthesized Mn_2O_3 were single phase tetragonal structure with grain size varying from 13-34 nm. Change in morphology of the nanostructures was observed with increasing amounts of CTAB but interestingly there was no change in phase. Also, as the amount of CTAB reached 100 mg, nanorods were visible. The UV-vis spectra show maximum absorbance in the UV region of the electromagnetic spectrum for all the samples. Also, extension into the visible range is noted which makes the samples suitable for making solar cells and transparent electrodes. The band gap studies were also consistent with the UV-vis results. The PL spectra demonstrated emission intensity quenching for Mn_2O_3 synthesized with highest amount of CTAB. This is particularly suitable for application as photocatalysts. Thus Mn_2O_3 can serve as excellent candidates for photocatalytic and supercapacitor devices.

ACKNOWLEDGEMENTS

Authors highly acknowledge DST-FIST (SR/FST/PSI-175/2012) project and Department of Chemistry, University of Kalyani for providing instrumental facility.

Declaration of interests

None

REFERENCES

1. Subramanian, V., Zhu, H., Vajtai, R., Ajayan, P. M., & Wei, B. Hydrothermal synthesis and pseudocapacitance properties of MnO_2 nanostructures. *Journal of Physical Chemistry* B, 109 (43), 20207–20214 (2005). DOI: 10.1021/jp0543330.
2. Chin, S. F., Pang, S. C., & Anderson, M. A. Self-assembled manganese dioxide nanowires as electrode materials for electrochemical capacitors. *Materials Letters*, 64(24). 2670–2672 (2010). DOI: 10.1016/j.matlet.2010.09.020.
3. Ding, Y. S., Shen, X. F., Gomez, S., Luo, H., Aindow, M., & Suib, S. L. Hydrothermal growth of manganese dioxide into three-dimensional hierarchical nanoarchitectures. *Advanced Functional Materials*, 16(4). 549–555 (2006). https://doi.org/10.1002/adfm.200500436.
4. Cushing, B. L., Kolesnichenko, & V. L., O'Connor, C. J. Recent advances in the liquid-phase syntheses of inorganic nanoparticles. *Chemical Review*, 104 (9). 3893-3946 (2004). DOI: 10.1021/cr030027b. PMID: 15352782.
4. Wang, X., & Li, Y. Rational synthesis of α-MnO_2 single-crystal nanorods. *Chemical Communications*, 0 (7). 764–765 (2002). DOI: 10.1039/B111723H.
5. Wu, J., Zhang, H., & Ma X. Synthesis and characterization of single crystalline MnOOH and MnO_2 nanorods by means of the hydrothermal process assisted with CTAB. *Materials Letters*, 60(29-30). 3895–3898 (2006). DOI: 10.1016/j.matlet.2006.03.136.

6. Li, W., Zhang, W., Reenen, S. V., Sutton, R. J., Fan, J., Haghighirad, A. A., Johnston, M. B., Wang, L., & Snaith, H. J. Enhanced UV-light stability of planar heterojunction perovskite solar cells with caesium bromide interface modification. *Energy & Environmental Science*, 9 (2). 490-498 (2016). DOI: 10.1039/C5EE03522H.
7. Khoon, T. N., Sebastian, P., Saman, A. B. S. Autonomous fire fighting mobile platform. *Procedia Engineering*, 41. 1145-1153 (2012). doi:10.1016/j.proeng.2012.07.294.
8. Kalubarme, R. S., Cho, M. S., Yun, K. S., Kim, T. S., & Park, C. J. Catalytic characteristics of MnO_2 nanostructures for the O_2 reduction process. *Nanotechnology*, 22 (39). 395402 (2011). doi: 10.1088/0957-4484/22/39/395402.
9. Cui, X., Wang, Y., Xu, Q., Sun, P., Wang, X., Wei, T., & Sun, Y. Carbon nanotube entangled Mn_3O_4 octahedron as anode materials for lithium-ion batteries. *Nanotechnology*, 28 (25). 255402 (2017). DOI: https://doi.org/10.1088/1361-6528/aa7239.
10. Patterson, A. L. The Scherrer formula for X-Ray Particle Size Determination. *Physical Review*, 56 (10). 978-982 (1939). DOI: https://doi.org/10.1103/PhysRev.56.978.
11. Jaganyi, D., Altaf, M., & Isaac, W. Synthesis and characterization of whisker shaped MnO_2 nanostructure at room temperature. *Applied Nanoscience*, 3(4). 329-333 (2013). DOI: https://doi.org/10.1007/s13204-012-0135-3.
12. Zhang, H., Zhu, H., & Sun, R. Fabrication of photocatalytic TiO_2 nanoparticle film on PET fabric by hydrothermal method. *Textile Research Journal*, 82 (8). 747–754 (2012). https://doi.org/10.1177/0040517511424526.
13. Tauc, J. Optical properties of amorphous semiconductors. *Amorphous and Liquid Semiconductors*. 159-220 (1974). DOI: https://doi.org/10.1007/978-1-4615-8705-7_4.
14. Wang, H-Z., Zhao, H-L., Liu, B., Zhang, X-T., Zuliang, D., & Wensheng, Y. Facile Preparation of Mn_2O_3 Nanowires by Thermal Decomposition of $MnCO_3$. *Chemical Research in Chinese Universities*, 26(1). 5-7 (2010).
15. Sharrouf, M., Awad, R., Roumie, M., & Marhaba, S. Structural, optical and room temperature magnetic study of Mn_2O_3 nanoparticles. *Materials Sciences and Applications*, 6. 850-859 (2015). DOI: http:// dx.doi.org/10.4236/msa.2015.610087.
16. Pandey, S., Thakur, M., Mewada, A., Anjarlekar, D., Mishra, N., & Sharon, M. Carbon dots functionalized gold nanorod mediated delivery of doxorubicin: Tri-functional nano-worms for drug delivery, Photothermal therapy and Bioimaging. *Journal of Materials Chemistry B*, 1 (38). 4972-4982 (2013). DOI: 10.1039/C3TB20761G.